Microbiology Associated with Disease on White Lotus (Nelumbo nucifera Gaertn.) and Application of Silver Nanoparticles for the Control of Plant Pathogens In vitro

VU, Nguyen Quang Hoang
Institute of Biotechnology, Hue University

QUANG, Hoang Tan
Institute of Biotechnology, Hue University

HONG, Hoang Thi Kim
Duy Tan University, Da Nang City

AGARIE, Sakae
Laboratory of Plant Production Physiology, Division of Agrobiological Science, Department of Bioresource Sciences, Faculty of Agriculture, Kyushu University

https://doi.org/10.5109/4797823

出版情報：九州大学大学院農学研究院紀要. 67 (2), pp.165-172, 2022-09. Faculty of Agriculture, Kyushu University
バージョン：
権利関係：

J. Fac. Agr., Kyushu Univ., **67** (2), 165–172 (2022)

Microbiology Associated with Disease on White Lotus (*Nelumbo nucifera* Gaertn.) and Application of Silver Nanoparticles for the Control of Plant Pathogens *In vitro*

Nguyen Quang Hoang VU[1], Hoang Tan QUANG[1], Hoang Thi Kim HONG[2]* and Sakae AGARIE

Laboratory of Plant Production Physiology, Division of Agrobiological Science,
Department of Bioresource Sciences, Faculty of Agriculture,
Kyushu University, Fukuoka 819–0395, Japan
(*Received May 8, 2022 and accepted May 10, 2022*)

Many bacterial and fungal pathogens are known to affect lotus, which limits both flower quality and yield production. Treatments such as pesticides can reduce pathogens but can result in resistance. This study was conducted to identify the most common fungal, and bacterial pathogens associated with leaf spot diseases of white lotus (*Nelumbo nucifera*). Molecular–based identification using ITS and 16 s ribosomal DNA sequences revealed that the isolates belonged to *Aspergillus aculeatus*, *Aspergillus fumigatus*, and *Klebsiella pneumoniae*. We evaluated the effect of silver nanoparticles against pathogens isolated from infected white lotus leaves. According to the findings, AgNPs have antifungal activities against these plant diseases at different concentrations of 0.1,1, 10, 20, and 30 mg/L. Treatment of 30 mg/L silver nanoparticles on PDA showed the highest inhibition rate of plant pathogenic fungi *Aspergillus* sp., and bacteria *Klebsiella pneumoniae*. Based on this result, it is possible to suggest that silver nanoparticles synthesized could be an efficient, safe, cost–effective, and affordable alternative to control disease in white lotus.

Key words: silver nanoparticles, antifungal, antibacterial, white lotus, pathogen plant

INTRODUCTION

Lotus (*Nelumbo nucifera* Gaertn.) is a potential perennial aquatic crop grown and consumed throughout Asia. The lotus plant is a symbol of purity in many countries. All parts of *N. nucifera* have been used for multiple purposes, such as food, ornamental, and herbal medicinal products (Zhu, 2017). Besides, it is particularly noted for its 1,300–year seed longevity. In particular, among the lotus cultivars, the white lotus is a traditional indigenous variety. It has a characteristic floral aroma, and its seeds are sweet, fleshy, and sticky. However, due to the competition of high–yielding lotus "Cao san" varieties and harmful pathogens appearing in lotus fields, the planting area gradually shrinks, leading to the risk of degeneration and loss of varieties.

Many bacterial and fungal pathogens affect lotus, limiting both lotus flower quality and plant yield production. Synthetic chemical fungicides and pesticides have been the most commonly applied method to control lotus diseases. However, the extensive use of fungicides and pesticides is causing environmental pollution (soil, water). These practices may have a harmful influence on beneficial non–target species in the ecosystem and negatively affect the biodiversity, contributing to the development of resistant pathogens, possibly posing a potential risk to human health, and threatening the food security of humans on this planet (Bartlett *et al.*, 2002). Therefore, there is a growing need to develop alternative approaches to control plant diseases. Recently, nanotechnology has drawn attention due to its numerous applications in health, pharmaceuticals, catalysis, energy, environmental sciences, and materials (Rajashekara, 2012). The metal nanoparticles demonstrated distinct and significantly different physical and chemical characteristics (Feldheim and Foss, 2002). This is true especially in regards to silver nanoparticles (AgNPs) with their large surface area which makes them attractive to addressing the challenges not met by the physical, chemical pesticides, and other biological control methods methods (Pulimi and Subramanian, 2016). Therefore, they have the potential to be widely used in agriculture as biocontrol agents to promote sustainable agriculture (Franci *et al.*, 2015; Rajwadi *et al.*, 2020).

The objectives of this study were to isolate and identify plant pathogens from the lake–grown white lotus regions and investigate the antifungal, antibacterial effect of green synthesized silver nanoparticles (AgNPs) to control lotus (*N. nucifera*) disease.

MATERIALS AND METHODS

Silver nanoparticles

A stock solution of silver nanoparticles (AgNPs) at a 40 mg/L (ppm) concentration was synthesized using green *Aloe barbadensis*. The synthesis of AgNPs using leaf extracts was done using the method described previously (Hong *et al.*, 2021). Solution contain different AgNPs were added to growth media to make different AgNPs concentrations (0.1, 1, 10, 20, 30 mg/L). All silver nanoparticle solutions and media were freshly prepared and used.

Collection of samples

From March to May 2021, lesion leaves were col-

[1] Institute of Biotechnology, Hue University, Vietnam
[2] Duy Tan University, Da Nang City, Vietnam
* Corresponding author: (E–mail: hoangtkimhong@duytan.edu.vn)

lected randomly, transported to the laboratory within a cooler, and then kept at 4°C until further use.

Fungal and bacterial pathogen isolation

Infected leaf lesions were cut into small pieces (5 × 5 mm) and sterilized with 1% sodium hypochlorite (NaClO) solution for 1 minute. The samples were washed three times with sterilized distilled water, then dried on sterile paper towels, plated on potato dextrose agar (PDA) medium (38 g PDA in 1 L distilled water), and incubated at 28 ± 2°C under 12 h photoperiod for 7 days. Pure cultures were obtained by transferring single hyphal tips to fresh PDA plates. Pure colonies were maintained in 70% glycerol solution and stored at –20°C.

Identification morphological of the fungal and bacterial isolates

The fungal isolates were used to identify their morphology, such as conidiophores, conidia's shape and size, and colony characters.

The morphological characteristics of bacterial isolates were analyzed for their microscopic features (Colour, shape, margin, transparency) through the Gram staining technique as described in Bergey's manual of systematic bacteriology.

Molecular identification of the fungal and bacterial isolates

The total DNA of isolates was extracted from infected leaves using the cetyltrimethyl ammonium bromide (CTAB) method for the PCR performance (Namba *et al*., 1993). The molecular identity of the fungal and bacterial isolate was determined using Polymerase chain reaction (PCR) amplification.

Fungal: The internal transcribed spacer (ITS) region of the ribosomal DNA was amplified and sequenced using primers

+ ITS1F (5'TCCGTAGGTGAACCTGCGG–3') and

+ ITS4 (5'–TCCTCCGCTTATTGATATGC–3') (White *et al*., 1990).

The ITS primers used were ITS–1F and ITS–4. The PCR amplification program consisted of 95°C for 5 min, followed by 35 cycles of 95°C for 1 min, 52°C for 30 seconds, 72°C for 1 min, and a final extension temperature of 72°C for 10 min, holding the temperature of 4°C.

Bacterial: 16sRNA amplification was performed using the primers

+ 27F (5'– AGAGTTTGATCCTGGCTCAG – 3') and

+ 1492R (5'–TACCTTGTTACGACTT–3').

PCR reaction was performed in a Thermal Cycler (Eppendorf, Germany), and the thermal program used for the PCR (polymerase chain reaction) was under the following conditions: initial denaturation at 92°C for 2 *min*, followed by 35 cycles with final denaturation at 92°*C* for 1 min, primer annealing at 50°*C* for 30 seconds, extension at 72°*C* for 90 seconds, and an additional 10 min at 72°C as a final extension. In addition, PCR product was subjected to electrophoresis on 1.2% (*w/v*) agarose gels in 1×TAE Buffer.

The sequences obtained were edited using the BioEdit 7.0 software, and consensus sequences were analyzed using the Molecular Evolutionary Genetics Analysis (MEGA X) software (Kumar *et al*., 2018). The similarity of the nucleotide sequences of the isolate was calculated using the BLAST algorithm (Basic Local Alignment Search Tool).

Pathogenicity test

The pathogenicity of purified isolates from the disease leaves lotus was tested on a concave white lotus and confirmed by Koch's postulates. Lotus were grown in pots under greenhouse conditions. Leaves of plant hosts were sprayed with spore suspensions of each of the isolates using a hand sprayer. Inoculated plants were then kept in a humid chamber and observed daily for disease symptoms

Evaluation of the antibacterial and antifungal activity of silver nanoparticles in the *in vitro*

An *in vitro* assay was carried out on PDA with 0.1, 1, 10, 20, and 30 mg/L of silver nanoparticles (AgNPs). Medium containing silver nanoparticles was poured into each 90 × 15 mm Petri dish. The media containing silver nanoparticles was incubated at room temperature. After 48 hours of incubation, an agar plug of 8 mm diameter containing fungi was inoculated simultaneously at the center of each Petri dish and incubated at 28 ± 2°C. The culture medium without silver nanoparticles was inoculated and cultured under the same conditions for the control treatment. The sizes of the colonies were measured after 5 days and each treatment was replicated.

The inhibition rate – IR (%) was calculated using the following formula: where R is the radial growth of fungi in the control plate, and r is the radial growth of fungi in silver nanoparticle treated plates.

$$IR = \frac{R-r}{R}\ x100$$

Antibacterial potency of synthesized AgNPs for inhibiting the growth of pathogens was tested *in vitro* on LB medium using the agar well–diffusion assay according to Bakht *et al*. (2011). The bacteria strains were spread on the LB medium. The disks were loaded with 50 μL of silver nanoparticles (0.1, 1, 10, 20, and 30 mg/L). The disks were then placed on the agar plate and incubated at 37°C for 24 h. The zone of inhibition was observed after 24 h of incubation. Three replicates were set at 30 ± 2°C.

RESULT AND DISCUSSION

Characteristics of concave white lotus

Concave white lotus was cultivated from mid–February 2021 to August 2021. Different stages of concave white lotus were observed in the field and photographed (Fig. 1). Concave white lotus has a medium–small tree size; young leaves are light green. Flower buds were white to pale green, oval long – shaped, seed pots flat. Lotus seed is elliptical. The pigment inside the

seed coat is white. The diameter of the leaves of white lotus is smaller than other lotus variety

The growth and development of the white lotus variety consists of the following main stages. There are two types of leaves in the vegetative phase: floating leaves and standing leaves. The floating leaf stage (S1) is the initial stage of development for the white lotus plant. When the floating leaves have covered most of the water's surface, the plant begins to generate standing leaves (S2). Following that, buds appear (S3) marking the beginning of the reproductive stage (50 – 60 days after planting). In early and mid–May, blooming starts (S4, S5 – approximately 65 – 75 days after planting). In late May and late June, they reach full bloom (90 – 120 days of planting). The last flowering period starts in mid–July (142 – 155 days). After 170 – 180 days (S8), their leaves turn yellow and wither, and the plant enters dormancy, seed pod has turned green. The seed pod will dry up and turn brown (S10). The entire growth period is 190 to 195 days.

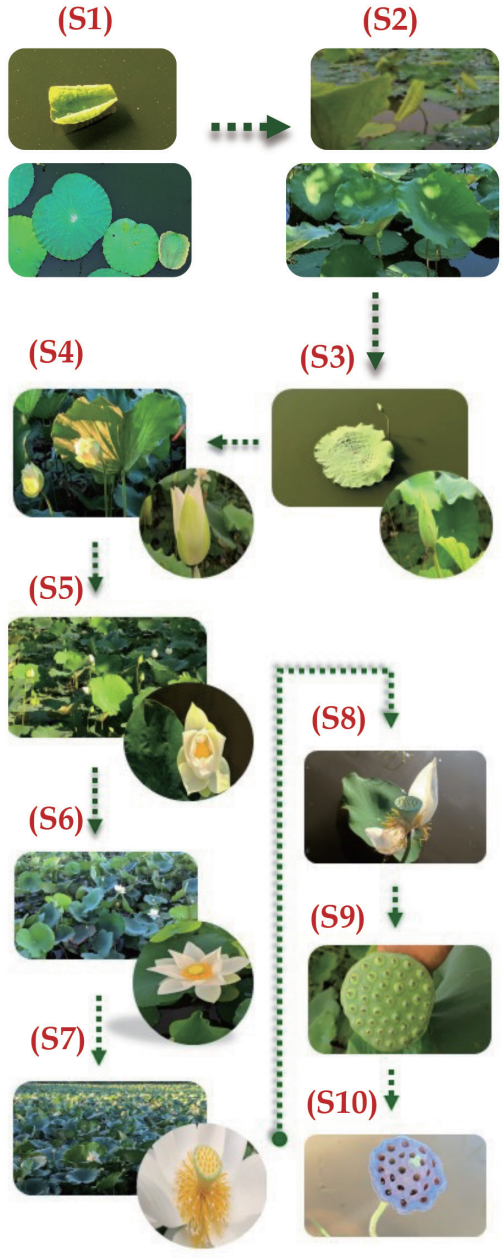

Fig. 1. Morphological, and physiological of concave white lotus (*Nelumbo nucifera*).
S1: floating leaf stage; S2: standing leaf stage; S3: bud appear; S4, S5, S6: Flower blooming; S7: Full bloom; S8: Petal begin fallen; S9: Seed pod has turned green and development; S10: Seed pod turns brown.

Disease symptoms, isolation and identification of the fungal, bacterial pathogen

Necrotic Brown Leaf disease with characteristic symptoms was represented by light brown, canker lesions that spread quickly. The initial stage of the blister blight infection process was marked by brown translucent spots with a yellow halo zone on the upper surface of leaves. At the end of the infection process, necrotic lesions on the leaves were observed. After 5 days, a colony of about 6.5 to 7.2 cm in diameter of STM1 isolates appeared on PDA, and it was brownish–black at the center and white at the edges (Fig. 2 D, E). Radial growth was 72.3 mm (recorded 5 days after injection on PDA). The conidiophore appeared pale brown, and the vesicles were not separate when observed through the microscope.

Brown leaf spot disease with typical symptoms consisted of small yellowish–brown spots, turning to dark brown or black after 7 –10 days infected. Lesion shapes tended to form radial streaks, from specks that became streaks running parallel to the leaf veins. For STM3 isolate from infected leaf (Fig. 3A), observed under the microscope, the isolate was characterized by green *Echinulate conidia*. Radial growth was 67.2 mm (recorded 5 days after injection on PDA). The mycelium differentiated into the septum branched and spore–

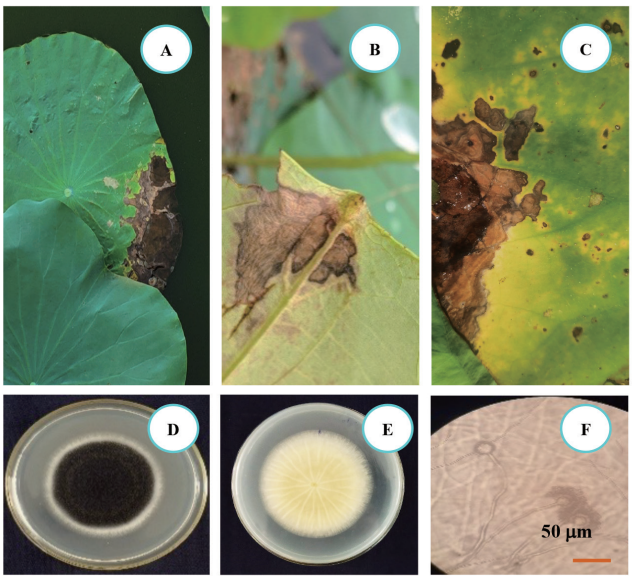

Fig. 2. Symptoms of Necrotic brown spot and pathogen isolate STCM1 (A), (B), (C): Disease symptoms of Necrotic Brown Spot observed in the lake; (D), (E): Colony morphology of STM1 on PDA, (F): Morphology of STCM1 in the microscope. Scale bar = 50 μm.

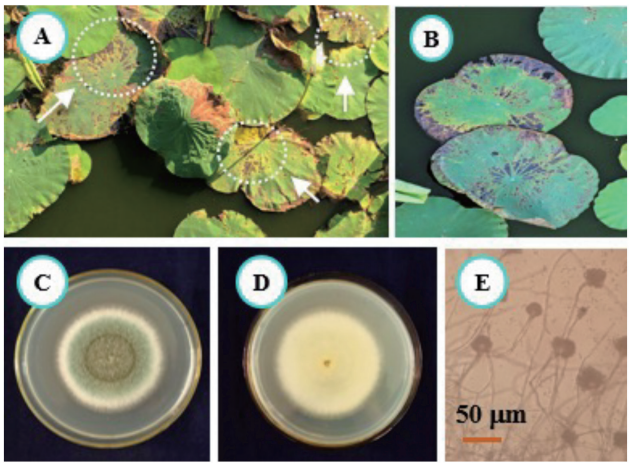

Fig. 3. Disease symptoms of Brown leaf spot and pathogen isolate STCM3
(A), (B): Disease symptoms of Brown leaf spot observed in the lake;
(C), (D): Colony morphology of STCM3 on PDA,
(F): Morphology of STCM3 in the microscope. Scale bar = 50 μm.

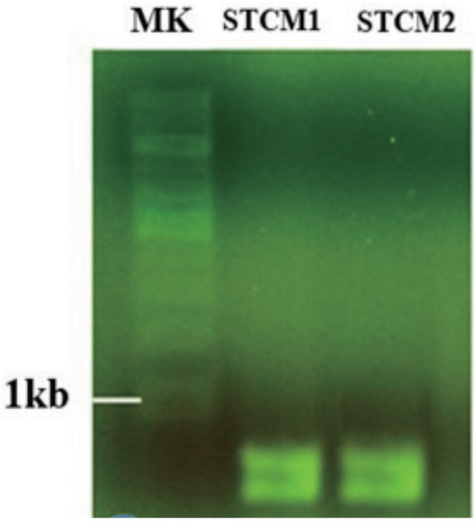

Fig. 4. Electrophoresis DNA total of STCM1, STCM3 isolate. MK: marker.

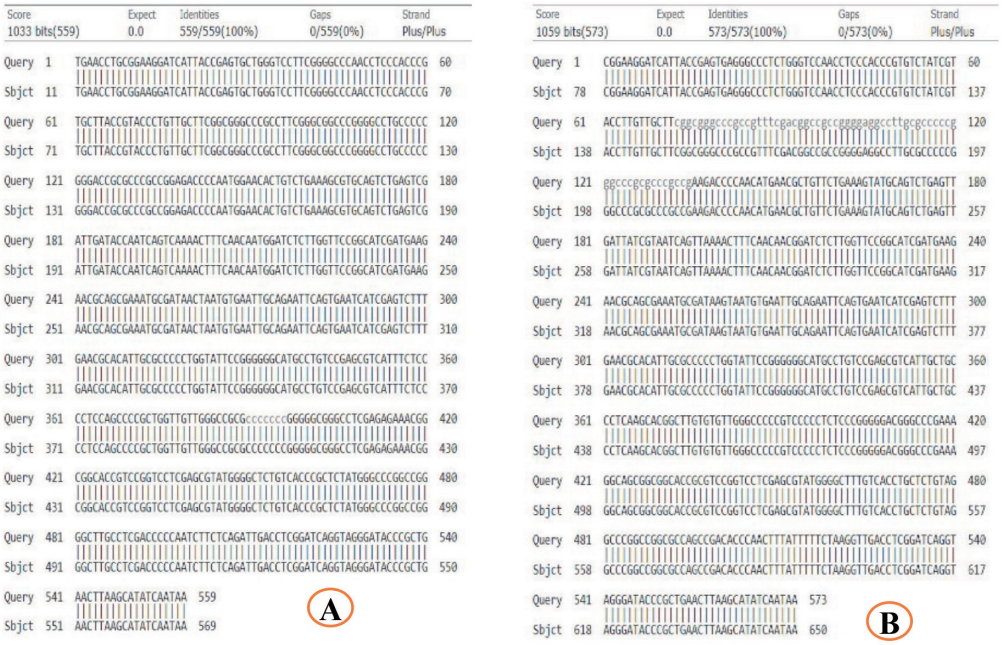

Fig. 5. Sequence of STCM1 (A). and Sequence STCM3 isolate (B).

forming stalks bearing spherical spores arranged in chains, with the spore stalks sunflower shaped (Fig. 3E). Initially, it was possible to identify the strains STCM1 and STCM3, which belong to *Aspergillus*.

The fungal–specific universal primer pairs ITS1 (forward) and ITS4 (reverse) effectively amplified the ITS region from DNA from all *Aspergillus* isolates. Capillary electrophoresis found sequence lengths ranging from 550 to 600 bp (Fig. 4). The morphological identification was corroborated by BLAST analysis of the ITS rDNA sequence data. The closest match (99 – 100 percent similarity) in the NCBI GenBank database was determined to be with distinct *Aspergillus* species. The results showed that the isolate STCM1 was 100% homologous to the ITS gene sequence of *Aspergillus aculeatus* (code: MN856264.1) (Fig. 5A), white STCM3 isolate was 100% homologous to the ITS gene sequence of *Aspergillus fumigatus* (Fig. 5B). (Code: MT597427.1).

The *Aspergillus aculeatus* was identified as a pathogen of grape berries in southwestern Ontario (Jarvis *et al.*, 1984). It is a wound pathogen that penetrates the berry via fractures induced by a partial detachment of fruits at the pedicel in tightly packed bunches, as well as splits and insect punctures. Other studies have reported the presence of *Botryodiplodia theobromae* and *Aspergillus aculeatus* – as pathogen causing soft rots of

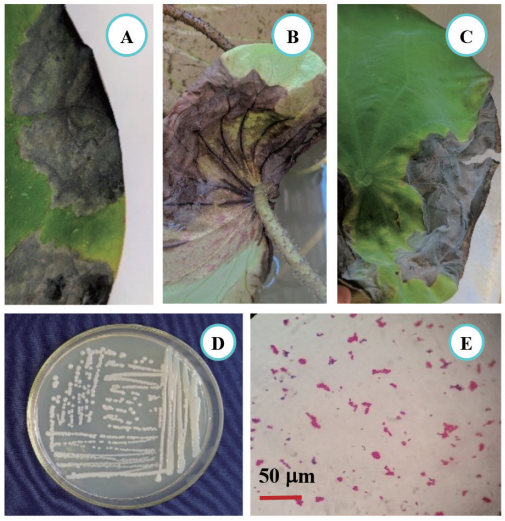

Fig. 6. Disease symptoms of Soft Rot and pathogen isolate STCV1
(A), (B), (C): Disease symptoms of Necrotic Brown Spot observed in lake;
(D): Colony morphology of STCV1 on LB, (E): Gram staining of STCV1.

Citrus fruits were grown on wheat offal medium (Adisa and Fojola, 1982).

Soft rot disease with typical symptoms includes soft rot, black color, necrosis, and water–soaked lesions at the edge of leaves and behind entire lotus leaves. We conducted isolates, and biochemical tests were performed to identify the pathogen from infected leaves. Strain STCV1 is a rod–shaped bacteria, non–flagellated, non–motile, and Gram–negative bacteria (Fig. 6E). Based on the morphological and biochemical test, the isolates were found to belong to Enterobacteriaceae.

After observing the colony morphology and microscopic visualizations, as shown in Fig. 6. STCV1 was further identified based on 16S rRNA sequence analysis. 27F–AGAGTTTGATCCTGGCTCAG was used as the forward primer, and the reverse primer was 1492R–GGTTACCTTGTTACGACTTT. Based on the 16 S rRNA sequence, bacterial isolates were classified into the genus *Klebsiella*. With comparative analysis of the 16 S rRNA gene, both morphological and biochemical, we identified the strain as *Klebsiella pneumoniae*, with 99.93% similarity.

Recently, *Klebsiella pneumoniae* is emerged as an important bacterial plant pathogen in Asia. The strain *Klebsiella pneumoniae* KpC4 was identified as a causative agent of bacterial top rot in maize, and has been observed in many areas of Yunnan province, China. In reports by Liu *et al.* (2015), it was reported to be a plant pathogen on onion bulbs causing internal tissue decay (soft rot) in Guangdong province, China. A previous report by Ajayasree and Borkar showed that *Klebsiella pneumoniae* causes root bark necrosis and wilt disease on pomegranate trees in India.

Antifungal and antibacterial activities of silver nanoparticles

The inhibitory effect of fungal mycelia growth was investigated in PDA medium containing different concentrations of 0.1, 1, 10, 20, and 30 mg/L (ppm) of silver nanoparticles (Fig. 7). The results were given in Fig. 7 and Fig. 8. There was a positive correlation between increased AgNPs concentration and antifungal efficacy. In addition, the size of the colonies decreased with the increased concentrations of silver nanoparticles. The results showed a very significant effect of synthesized silver nanoparticles on the mycelium growth of *Aspergillus* sp. More than 95% of the inhibitory effect on fungal growth was demonstrated on the *Aspergillus* sp. (96.72% with *Aspergillus aculeatus*, 97.22% with *Aspergillus fumigatus*) treated with AgNPs 30 mg/L. However, no significant differences were found among the control, 0.1, and 1 mg/L concentrations, with 0, 0.68, and 1.38% inhibition rates, respectively. In *Aspergillus fumigatus*, there were no significant differences when treated with 0.1 mg/L and 1 mg/L of silver nanoparticles with approximately 10% growth inhibitory (9.83%, 11,47%, respectively).

In general, the inhibition increased with the concentration of silver nanoparticles. These findings are in agreement with those obtained by Park *et al.* (2006); Kim *et al.* (2009); and Fatimah Al–Otibi (2021) reported

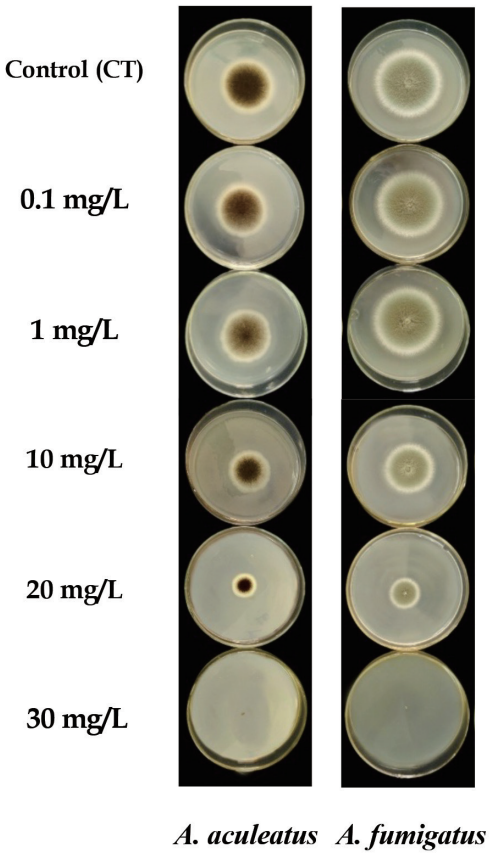

Fig. 7. Inhibition effect of silver nanoparticles (AgNPs) against fungal pathogen on PDA *in vitro*. Images were captured after culture plates had been incubated for 5 days at 28°C.

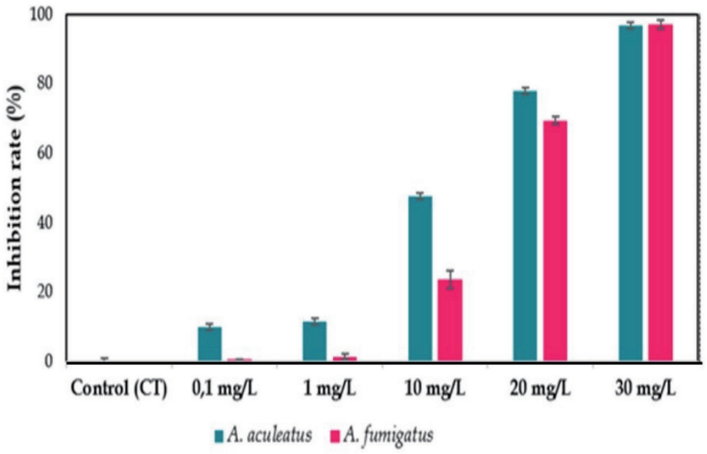

Fig. 8. Inhibition rate (%) of silver nanoparticles (AgNPs) against fungal pathogen.

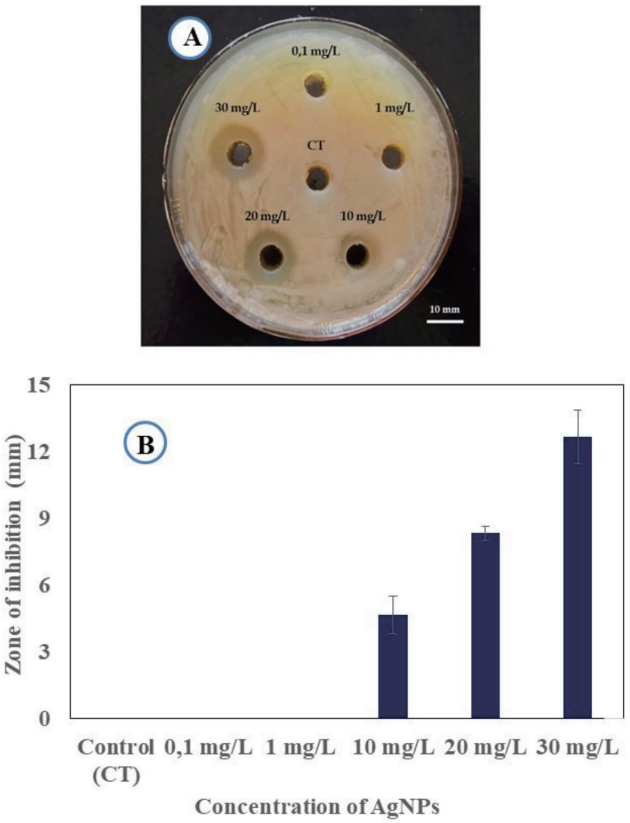

Fig. 9. Inhibition effect of silver nanoparticles (AgNPs) against bacterial pathogen.
(A). Zone of inhibition of silver nanoparticles; (B). bar graph showing zone of inhibition introduced by AgNPs against *Klebsiella pneumonia*. Images were captured after plates had been incubated for 24 hours at 35°C.

that Ag ions and silver nanoparticles had a significant effect on plant pathogenic fungi, *Bipolaris sorokiniana*, *Fusarium solani*, *Raffaelea* species, and Colletotrichum species.

In this study, we also conducted a detailed study on the role of concentration for the antibacterial activity of silver nanoparticles against *Klebsiella pneumoniae* – caused soft rot disease in *N. nucifera* (*cv*. concave white lotus). Fig. 9A, 9B shows the resulting zone of inhibition observed against *Klebsiella pneumoniae*. The larger inhibition zone was detected for treated with AgNPs at 10 mg/L, 20 mg/L, and 30 mg/L concentrations. No detected antibacterial "halo" with treated AgNPs at lower concentrations of 10 mg/L (0.1 mg/L, 1 mg/L)

Management of fungal and bacterial diseases on crops is economically essential. There have been numerous previous reports of silver nanoparticles' antimicrobial, antifungal use in treating *Escherichia coli*, *Staphylococcus aureus*, *Bacillus subtilis*, *Klebsiella mobilis*, *Mycobacterium tuberculosis*, and *Candida albicans*. This study confirms that silver nanoparticles have significant inhibitory effects on colony formation from conidia of *Aspergillus fumigatus*, *Aspergillus aculeatus*, and *Klebsiella pneumonia* – a pathogens–caused disease of a white lotus. The exact mechanisms of AgNPs against plant pathogens (bacteria, fungi) remain unknown. However, many studies have found that the electrostatic attraction between microorganisms; negatively charged cell membranes, such as bacteria, viruses, and fungus: and, positively charged nanoparticles play a critical role in the antibacterial activity of nanomaterials. Therefore, it was believed that silver nanoparticles with large surface areas could quickly form Ag+, binding to functional groups (–SH) of proteins and this resulted in protein denaturation. Besides, the antimicrobial activities of silver nanoparticles may result from a loss or inhibition of replication activity that inactivates the cellular proteins and enzymes of the pathogens (Feng QL, 2000).

The results have shown that silver nanoparticles can inhibit the growth and development of bacterial and fungal strains. Based on the findings of this study, silver nanoparticles are one of the most effective solutions for disease management on the white lotus (*Nelumbo nucifera*) *in vivo*. AgNPs green synthesis is considered less harmful, toxic, and cost–effective than other methods. This study promises the application of silver nanomaterials in the prevention and control of diseases on lotus plants caused by microbial agents, improving both the quality and quantity of white lotus.

CONCLUSION

This study has isolated and identified fungal and bacterial (*Aspergillus fumigatus*, *Aspergillus aculeatus*, *Klebsiella pneumoniae*) caused diseases in white lotus (*Nelumbo nucifera*). Endophytes can act as potential pathogens of white lotus, capable of inflicting severe damage to cultivate. Silver nanoparticles show significant antibacterial activity, antifungal against plant pathogens. Therefore, AgNPs could be a good alternative for development as an antibacterial, antifungal agent in this lotus variety. AgNPs can lead to valuable findings in various applications in agriculture, providing a novel and sustainable alternative in the food and agriculture sectors for disease management and control.

AUTHOR CONTRIBUTIONS

Nguyen Quang Hoang Vu contributed to the study conception, design, material and sample preparation, and analysis. The disease symptoms, isolation and identification of the fungal, bacterial pathogen of the manuscript was written by Hoang Tan Quang. Hoang Thi Kim Hong designed and supervised the research work. Sakae Agarie critically reviewed the manuscript with valuable suggestions comments. All authors read and approved the final manuscript.

ACKNOWLEDGEMENTS

Nguyen Quang Hoang Vu was funded by Vingroup Joint Stock Company and supported by the Domestic PhD Scholarship Programme of Vingroup Innovation Foundation (VINIF), Vingroup Big Data Institute (VINBIGDATA), code [VINIF.2021.TS.145].

REFERENCES

Adisa, V. A., and A. O. Fajola 1982 Pectinolytic enzymes associated with the soft rots of Citrus sinensis caused by *Aspergillus aculeatus* and *Botryodiplodia theobromae*. *Mycopathologia*, **77**(1): 47–50. https://doi.org/10.1007/BF00588657

Aguilar–Méndez, M. A., Martín–Martínez, E. S., Ortega–Arroyo, L., Cobián–Portillo, G., and E. Sánchez–Espíndola 2011 Synthesis and characterization of silver nanoparticles: Effect on phytopathogen *Colletotrichum gloesporioides*. *Journal of Nanoparticle Research*, **13**(6): 2525–2532. https://doi.org/10.1007/s11051–010–0145–6

Akpinar, I., Unal, M., and T. Sar 2021 Potential antifungal effects of silver nanoparticles (AgNPs) of different sizes against phytopathogenic *Fusarium oxysporum* f. sp. radicis–lycopersici (FORL) strains. *SN Applied Sciences*, **3**(4). https://doi.org/10.1007/s42452–021–04524–5

Aladame, N 1987 Bergey's manual of systematic bacteriology. *Annales de l'Institut Pasteur / Microbiologie*, **138**(1). https://doi.org/10.1016/0769–2609(87)90099–8

. Al–Otibi, F., Perveen, K., Al–Saif, N. A., Alharbi, R. I., Bokhari, N. A., Albasher, G., Al–Otaibi, R. M., and M. A. Al–Mosa 2021 Biosynthesis of silver nanoparticles using Malva parviflora and their antifungal activity. *Saudi Journal of Biological Sciences*, **28**(4): 2229–2235. https://doi.org/10.1016/j.sjbs.2021.01.012

An, C., Sun, C., Li, N., Huang, B., Jiang, J., Shen, Y., Wang, C., Zhao, X., Cui, B., Wang, C., Li, X., Zhan, S., Gao, F., Zeng, Z., Cui, H., and Y. Wang 2022 Nanomaterials and nanotechnology for the delivery of agrochemicals: strategies towards sustainable agriculture. In *Journal of Nanobiotechnology*, **20**(1): 11. https://doi.org/10.1186/s12951–021–01214–7

Ajayasree, T. S., S. G. Borkar 2018 Biochemical characteristics of plant pathogenic *Klebsiella pneumoniae* causing root bark necrosis and wilt in pomegranate. *Journal of Applied Biotechnology and Bioengineering*, **5**(4): 222–225 https://doi.org/10.15406/jabb.2018.05.00141

Bartlett, D. W., Clough, J. M., Godwin, J. R., Hall, A. A., Hamer, M., and B. Parr–Dobrzanski 2002 The strobilurin fungicides. In *Pest Management Science*, **58**: 649–62. https://doi.org/10.1002/ps.520

Chen, C. C., Chen, Y. Y., Yeh, C. C., Hsu, C. W., Yu, S. J., Hsu, C. H., Wei, T. C., Ho, S. N., Tsai, P. C., Song, Y. D., Yen, H. J., Chen, X. A., Young, J. J., Chuang, C. C., and H. Y. Dou 2021 Alginate–Capped Silver Nanoparticles as a Potent Anti–mycobacterial Agent Against *Mycobacterium tuberculosis*. *Frontiers in Pharmacology*, **12**: 746496. https://doi.org/10.3389/fphar.2021.746496

Feng, Q. L., Wu, J., Chen, G. Q., Cui, F. Z., Kim, T. N., and J. O. Kim 2000 A mechanistic study of the antibacterial effect of silver ions on *Escherichia coli* and *Staphylococcus aureus*. *Journal of Biomedical Materials Research*, **52**(4): 662–668. https://doi.org/10.1002/1097–4636(20001215)52:4<662::AID–JBM10>3.0.CO;2–3

Franci, G., Falanga, A., Galdiero, S., Palomba, L., Rai, M., Morelli, G., and M. Galdiero 2015 Silver nanoparticles as potential antibacterial agents. In *Molecules*, **20**(5): 8856–8874. https://doi.org/10.3390/molecules20058856

He, X., Deng, H., and H. M. Hwang 2019 The current application of nanotechnology in food and agriculture. In *Journal of Food and Drug Analysis*, **27**(1): 1–21. https://doi.org/10.1016/j.jfda.2018.12.002

Hong, H. T. K., Vu, N. Q. H., Hanh, N. T. N., Ha, T. T., and L. Q. T. Dung 2021 Study on the *In vitro* and *In vivo* Antifungal Activities of Nano–silver against *Mycoleptodiscus indicus* causing Leaf Blight on Lotus in Vietnam. *Indian Journal of Agricultural Research*. https://doi.org/10.18805/ijare.af–685

Jarvis, W. R 1984 Bunch Rot of Grapes Caused by *Aspergillus aculeatus*. *Plant Disease*, **68**(1): 718–719. https://doi.org/10.1094/pd–68–718

Kim, J. S., Kuk, E., Yu, K. N., Kim, J. H., Park, S. J., Lee, H. J., Kim, S. H., Park, Y. K., Park, Y. H., Hwang, C. Y., Kim, Y. K., Lee, Y. S., Jeong, D. H., and M. H. Cho 2007 Antimicrobial effects of silver nanoparticles. *Nanomedicine: Nanotechnology, Biology, and Medicine*, **3**(1): 95–101. https://doi.org/10.1016/j.nano.2006.12.001

Kim, S. W., Jung, J. H., Lamsal, K., Kim, Y. S., Min, J. S., and Y. S. Lee 2012 Antifungal effects of silver nanoparticles (AgNPs) against various plant pathogenic fungi. *Mycobiology*, **40**(1): 53–58. https://doi.org/10.5941/MYCO.2012.40.1.053

Kim, S. W., Kim, K. S., Lamsal, K., Kim, Y. J., Kim, S. bin, Jung, M., Sim, S. J., Kim, H. S., Chang, S. J., Kim, J. K., and Y. S. Lee 2009 An *in vitro* study of the antifungal effect of silver nanoparticles on oak wilt pathogen Raffaelea sp. *Journal of Microbiology and Biotechnology*, **19**(8): 760–764 https://doi.org/10.4014/jmb.0812.649

Kumar, S., Stecher, G., Li, M., Knyaz, C., and K. Tamura 2018 MEGA X: Molecular evolutionary genetics analysis across computing platforms. *Molecular Biology and Evolution*, **35**(6): 1547–1549. https://doi.org/10.1093/molbev/msy096

Liu, S., Lv, M., Gu, Y., and J. Zhou 2015 First report of bulb disease of onion caused by Subramanian, *of Science and Research (IJSR)*, **14**(7)

Pulimi, M., and S. Subramanian 2016 *Nanomaterials for Soil Fertilisation and Contaminant Removal*. In: Ranjan, S., Dasgupta, N., Lichtfouse, E. (eds) Nanoscience in Food and Agriculture 1. Sustainable Agriculture Reviews, Vol.20, Springer, Cham, pp: 229–246. https://doi.org/10.1007/978–3–319–39303–2_8

Rajwade, J. M., Chikte, R. G., and K. M. Paknikar 2020

Nanomaterials: new weapons in a crusade against phytopathogens. In *Applied Microbiology and Biotechnology*, **104**(4): 1437–1461. https://doi.org/10.1007/s00253–019–10334–y

Sadeghi, B., Jamali, M., Kia, S., Amini, a, and S. Ghafari 2010 Synthesis and characterization of silver nanoparticles for antibacterial activity. *Scanning Electron Microscopy*, **1**(2): 119–124 https://www.sid.ir/en/journal/ViewPaper.aspx?id=194433

Zhu, F 2017 Food Hydrocolloids Structures, properties, and applications of lotus starches. *Food Hydrocolloids*, **63**, 332–348 https://doi.org/10.1016/j.foodhyd.2016.08.034